Korean J. Chem. Eng., 35(6), 1319-1327 (2018)
DOI: 10.1007/s11814-018-0039-3

pISSN: 0256-1115
eISSN: 1975-7220

A hydrogel-coated membrane for highly efficient separation of microalgal bio-lipid

Jihye Shin*, Hogi Kim*, Heeyeon Moon*, Moo Jin Kwak*, Seula Oh*, Youngmin Yoo*, Eunjung Lee*, Yong Keun Chang*,,†, and Sung Gap Im*,†**

*Department of Chemical and Biomolecular Engineering, KAIST, Daejeon 34141, Korea
**Advanced Biomass R&D Center, Daejeon 34141, Korea
(*Received 20 November 2017 • accepted 23 February 2018*)

Abstract−A cross-linked hydrogel-coated membrane was fabricated to achieve simple but highly efficient separation of bio-lipids directly from an aqueous microalgal culture medium. The membrane is composed of a stainless steel membrane coated conformally with a cross-linked hydrogel, poly(2-hydroxyethyl methacrylate) (pHEMA), synthesized by a photo-initiated chemical vapor deposition (piCVD) process. The pHEMA-coated membrane has hydrophilicity and underwater-oleophobicity for efficient separation of a bio-lipid-in-hexane/water mixture by gravity. The conformal pHEMA film-coated membrane enables extremely high oil rejection performance with intrusion pressure of 6.1 kPa and water permeation flux of 6.5×10^3 L m^{-2} h^{-1}, with excellent separation efficiency greater than 98.0%.

Keywords: Membrane, Hydrophilic, Underwater-oleophobic, Cross-linked Hydrogel, Bio-lipid Separation, Photo-initiated Chemical Vapor Deposition (piCVD)

INTRODUCTION

Searching for alternative energy sources such as biomass, water, wind, solar, and geothermal powers has drawn huge interest in an efforts to replace the existing fossil fuels, which have many problems including unsustainability, unstable price variation, and environmental pollution [1,2]. Among these energy sources, biomass is regarded as a promising candidate energy source due to its high potential capability of providing clean energy without generating any critical environmental issues [3-5]. In particular, microalgal biomass is advantageous for biofuel production on a large-scale due to the high lipid content, rapid growth rate, and high biodiesel productivity [6-8]. However, the production of microalgae-derived biofuels are still suffers from the high production cost, which must be reduced substantially by developing a simple but highly efficient process for cost-competitive biofuel production from microalgal biomass [9].

The whole process to obtain microalgal biofuel largely consists of four key steps of cultivation, harvesting, extraction, and conversion [10]. In particular, in the course of harvesting and extraction, dewatering is a unique step required in microalgal biomass production since microalgae are aquatic organisms and a huge amount of water must be removed from the cultivated microalgae for the production of microalgal biofuel [11]. Most importantly, the dewatering step is one of the most energy-intensive processes, and is responsible for about 40% of total production cost [12]. Therefore, the dewatering cost must be scaled down substantially to make microalgal biofuel production economically feasible. For harvesting, a flocculation method using chemical coagulants has been attempted due to its high efficiency, and the separation of biomass from culture medium using eco-friendly coagulant of rice starch was reported recently [13]. However, to reduce the processing steps, methods for direct extraction of bio-lipid from wet microalgal biomass have been investigated intensively [14,15]. The usually employed method for wet extraction involves cell disruption of wet microalgae mostly by solvent treatment, followed by solvent extraction of bio-lipids released from the disrupted microalgal cells. For efficient and eco-friendly biofuel production, pulsed electric field pretreatment and bio-solvents were also investigated in bio-lipid extraction [16,17]. However, consequently, the wet extraction process generates a mixture of the extracted bio-lipid phase dissolved in an organic solvent and the aqueous culture medium with the disrupted microalgal cell debris, and these components should be separated from each other with minimum cost [10]. A floatation method using density difference is generally used to separate the lipid-in-organic solvent phase from the aqueous culture medium. However, the floatation-based separation process must be operated in a batch manner, and the method is extremely time-consuming to induce phase separation. Most importantly, a huge amount of lipid content might be lost in the floatation-based separation process, which critically limits the application of this separation method to mass production [18].

Membrane-based separation could provide a simple but powerful method for efficient collection of bio-lipids with minimal energy input. The membrane-based separation of an oil/water mixture is an eco-friendly, scalable method operable in a continuous manner due to its high selectivity, short process time, energy efficiency, and simplicity [19]. The membrane-based separation involves the selective permeation of one phase while blocking penetration of the other phase to achieve separation of two phases in a mixture. In the separation of a bio-lipid-containing solvent phase from an aqueous culture medium, two possible routes can be considered: adapting a water-permeating membrane and an oil-permeating membrane while blocking the other phase [20-23]. Chloroform has been con-

†To whom correspondence should be addressed.
E-mail: sgim@kaist.ac.kr, changyk@kaist.ac.kr

sidered as a lipid-extracting solvent due to its high extracting performance, and a membrane-based separation of a lipid-containing solvent phase had been demonstrated by using an oil-permeating membrane [24]. However, recent reports have commonly indicated that chloroform cannot be applied to large-scale lipid extraction due to its high toxicity [25,26]. Instead, hexane is regarded as one of the most promising solvent candidates for lipid extraction due to its relatively low toxicity compared to chloroform, low affinity to non-lipid contaminants, and high selectivity to neutral lipids [27]. The prominent difference between hexane and chloroform is the density; hexane is lighter and chloroform is heavier than water. Therefore, water-penetrating membrane is more suitable to drain water through the membrane by gravity-driven separation in hexane-based extraction. Notably, gravity-driven separation does not require any additional power for membrane-based separation. The gravity-driven method can also be highly efficient as far as the method allows high permeation flux through the membrane. Compared to a water-permeating membrane, an oil-permeating membrane meanwhile suffers from an unavoidable oil fouling problem due to its intrinsic oleophilic nature, leading to low recyclability of the membrane [28]. For efficient, gravity-driven oil phase separation, various methods have been attempted to fabricate water-permeating membranes, mostly involving surface modification of the membrane to incorporate hydrophilic and hygroscopic properties to the membrane [29-32]. However, most liquid phase-based surface modification methods suffer from non-conformal surface coverage and pore clogging, which significantly degrade the separation performance of the membrane. Most importantly, for the fabrication of a water-permeating surface, hydrophilic and hygroscopic surface modification is critical. However, the functionalities are prone to damage by various solvents, especially water. For example, the functionalities can be dissolved out, or excessively swollen, which might substantially degrade the performance of the membrane [33,34]. To mitigate this problem, the hydrophilic surface functionalities must be stabilized. In this regard, it is necessary to develop a versatile surface modification method to generate a hydrophilic surface with enhanced chemical and mechanical stability, but the fabrication process itself must be simple and reliable.

In this work, we suggest a novel hydrophilic water-permeating membrane with increased permeation flux for the separation of lipids extracted in hexane from a microalgal culture medium to satisfy the requirements for mass production of microalgal biofuel. For this purpose, a porous steel-use-stainless (SUS) membrane was coated conformally with a cross-linked hydrogel composed of poly(2-hydroxyethyl methacrylate) (pHEMA). The polymer film was synthesized directly on the SUS membrane in a simple, one-step manner via photo-initiated chemical vapor deposition (piCVD) to assign hydrophilic and underwater-oleophobic properties to the membrane surface. In the piCVD process, the corresponding monomer, 2-hydroxyethyl methacrylate (HEMA), decomposes into radical species by UV irradiation (254 nm) to form a cross-linked pHEMA by free radical polymerization without the use of a photo-initiator [35]. The pHEMA film maintained the hydrophilic -OH functionalities and the cross-linking network of the hydrophilic polymer dramatically improved the chemical and mechanical stability of the hydrogel film on the SUS membrane. The piCVD process provided a thin, uniform, and conformal polymer coating to preserve the inherent porous structure of the membrane while imparting selective wettability onto the membrane, making the pHEMA-coated SUS membrane highly water-absorbing and underwater-oleophobic [36-38]. Simple and effective separation of the bio-lipid phase from the aqueous culture medium was achieved by using the surface-modified membrane. Separation of an olive oil-in-hexane and water mixture as a model system using the hydrogel-coated membrane was attempted, where the olive oil, mimicking the microalgal bio-lipid, remained in the retentate phase while water permeated rapidly and completely through the membrane. The separation performance was estimated by the permeation flux, separation efficiency, and intrusion pressure. Finally, the separation of a mixture of real microalgal bio-lipids and a culture medium was also attempted by the hydrogel-coated membrane. Furthermore, recyclability of the membrane, which originated from its outstanding chemical and mechanical stability was demonstrated. Application of the water-permeating pHEMA-coated membrane with high separation performance to the biomass separation process will greatly reduce the lipid loss and process time, and promote mass production of microalgal biofuels with economic feasibility.

MATERIALS AND METHODS

1. Synthesis of pHEMA via piCVD

pHEMA was synthesized from its corresponding monomer, HEMA (95%, TCI Chemicals) via piCVD process. Si wafers (Siltron, Inc.), glass slides (Marienfeld, Inc.), and steel-use-stainless (SUS) membrane with the mesh number of 1250 were used as the substrate materials. Substrates were located in a piCVD chamber (Daeki Hi-tech, Inc.). The substrate temperature was maintained in the range of 25 to 35 °C. HEMA was heated up to 75 °C to vaporize the monomer and introduced into the chamber at the flow rate of 0.91 standard cubic centimeters per minute (sccm). The chamber pressure was set to 90 mTorr and 254 nm of UV irradiation (VL-6-L.C, Vilber Lourmat) with the light intensity of 400 μW cm^{-2} was applied to the piCVD chamber through the quartz view port. The total distance from the substrate to UV light source was 88 mm. All of the chemicals in this study were used as received without further purification.

2. Characterization of pHEMA

FT-IR spectra were obtained by ALPHA FTIR (Bruker Optics). The static WCAs and underwater OCAs were measured by a contact angle analyzer (Phoenix 150, SEO, Inc.). The volume of an individual droplet was 10 μL. For measuring underwater OCAs, 1,2-dichloroethane (99.8%, Sigma Aldrich) was used. Thickness reduction was estimated by the ratio of the pHEMA film thickness before and after soaking in DI water for 24 h. After soaking in DI water, the pHEMA-coated Si wafer was dried in ambient condition for a day. The film thickness was obtained by spectroscopic ellipsometry at an incident angle of 70°. The obtained data was fit to a Cauchy model (alpha SE, J.A. Woollam Co., Inc.). Surface image and morphology were observed using field emission SEM (FE-SEM) (SU5000, Hitachi) and atomic force microscopy (AFM) (XE-100, Park system). The pore diameter and size distribution were measured by capillary flow porometer (CFP-1500AEL, Porous Materi-

als Inc.). Galwick solution was used to fully wet on the membrane and N_2 gas was used to burst the blocked pores by galwick solution. The swelling ratio of the cross-linked hydrogel-coated membrane was obtained by measuring the mass of the membrane before and after soaking the membrane in DI water for a designated time. The swelling ratio was calculated using the following equation [39]:

$$\text{Swelling ratio (\%)} = (M_s - M_d)/M_d \times 100$$

where M_s and M_d were the mass of swelled and dried membrane, respectively. The mass of swelled membrane was measured after removing excessive water on the surface by filter paper. The solvent resistance of pHEMA-coated membrane was determined by measuring the WCAs after soaking in each solvent (Deionized water, isopropyl alcohol (Duksan), hexane (Daejung), lipid-in-hexane and culture medium) for 24 h. The solvent-treated samples were rinsed with acetone (Duksan) and isopropyl alcohol, and then dried for 30 min on a hot plate of 50 °C.

3. Model Mixture Separation Test

Before the separation test, the pHEMA-coated membrane was fully soaked in DI water for 10 min. The water absorbed membrane was placed between the two glass cylinders (diameter: 37.3 mm) sealed with a clamp to prevent leakage. The model mixture consisted of 30 mL olive oil-in-hexane (1.35 g L^{-1}) and 70 mL water. The olive oil-in-hexane phase was dyed with Oil red O (Sigma Aldrich) for better visualization. The mixture was poured onto the apparatus equipped with pHEMA-coated membrane. The permeation flux (F) was calculated by measuring the time for a certain amount of liquid to pass through the membrane with the equation below [40]:

$$F = \frac{V}{S \cdot t}$$

where V is the volume of liquid passing through the membrane, S is the area of the membrane, and t is the time for the liquid to penetrate through the membrane. The intrusion pressure (P) of the pHEMA-coated SUS membrane was estimated using the following equation [41]:

$$P = \rho g h_{max}$$

where ρ is the density of oil, g is the acceleration of gravity, and h_{max} is the maximum height of the oil before oil leakage starts. To calculate the separation efficiency, total lipid was obtained by measuring the mass of olive oil before and after the separation. The mass of glass tube was first measured and 5 mL of olive oil-in-hexane was filled in each glass tube. The olive oil-in-hexane in glass tube was heated up to 50 °C of water bath for 12 h. The hexane was vaporized away to leave olive oil only. More than three separate samples were measured and averaged to determine the oil content. The amount of water in olive oil-in-hexane before and after the separation was measured by Karl Fischer method (ISO 760:2007) to check the remaining water content in oil phase after the separation [42].

4. Microalgae Strain, Cultivation, Solvent Extraction and Removing Cell Debris

The microalgal strain *Chlorella sorokiniana*. HS1 (Chloland) was cultivated by open-pond cultivation, containing 20 g L^{-1} of water soluble fertilizer (Eco-sol, 25-9-18, Hannong). The fertilizer consisted of 25.0% of total nitrogen (N), 9.0% of phosphorous (P_2O_5), 18.0% of potassium (K_2O), and micro nutrients: 250 ppm of iron (Fe), 250 ppm of manganese (Mn), 500 ppm of boron (B), 75 ppm of zinc (Zn), 75 ppm of copper (Cu), and 5 ppm of molybdenum (Mo). The microalgae was concentrated using a centrifuge (Supra 22K, Hanil) at 4,000 rpm for 5 min and stored at −70 °C for 24 h. To collect the dried samples, the frozen samples were dried by freeze-drying (Ilshin) for up to three days. Prior to lipid extraction, 2 N of sulfuric acid solution containing 10 g L^{-1} of microalgae was heated in an autoclave at 120 °C for 1 h for cell disruption. After cell disruption, hexane (98%, sigma Aldrich) was added at a volume ratio of 1 : 1 and solvent extraction was carried out at room temperature for 12 h. The lipid-extracted cell debris were filtered with a paper filter.

5. Bio-lipid Separation

Similar to the model mixture separation test method, the hexane with bio-lipid was separated from culture medium by the sep-

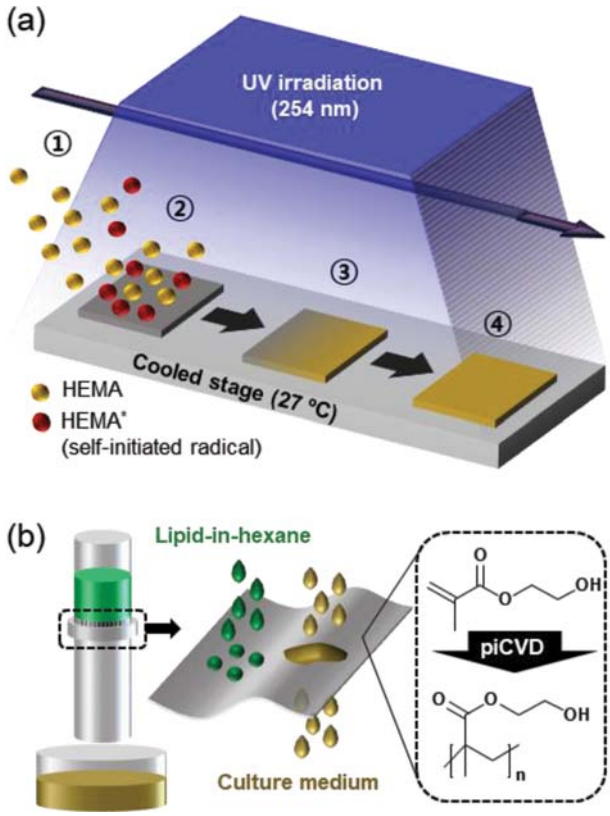

Fig. 1. (a) A schematic illustration of pHEMA synthesis via piCVD. First, HEMA monomer was injected into the reactor (①). The monomer was then adsorbed on the cooled substrate and the self-initiated radical, HEMA*, was formed by UV irradiation (②). The collisions among HEMA* and HEMA occurred cause free-radical polymerization on the surface of the membrane (③), and finally, the thin film pHEMA was coated on the substrate (④). (b) A schematic image of pHEMA-coated membrane for lipid-in-hexane separation from a culture medium. The water phase, the microalgal culture medium, can pass though the membrane while the oil phase, lipid-in-hexane, was blocked by the membrane.

aration apparatus with pHEMA-coated membrane. The bio-lipid mixture consisted of 30 mL lipid-in-hexane and 70 mL culture media. The permeation flux, intrusion pressure, total lipid, and water content in oil phase were all measured as described above. Before and after the separation, each lipid-in-hexane phase was also analyzed by GC. In brief, about 10 mL of lipid-in-hexane was transferred to a Teflon-sealed tube, followed by mixing vigorously for 30 s, and then the hexane was dried through nitrogen purge. 2 mL of chloroform-methanol mixture (2 : 1, v/v) was added into the dried lipid and mixed vigorously for 10 min. An additional 1 mL chloroform containing 0.5 mg heptadecanoic acid (C17:0) as an internal standard and 300 µl sulfuric acid were added. The mixture was heated at 100 °C for 20 min for complete transesterification of extracted lipids into fatty acid methyl esters (FAMEs). The organic phase was separated by adding 1 mL of DI water, then recovered by centrifugation at 4,000 rpm for 10 min. The amount of FAME was quantified by gas chromatography (Agilent 7890B GC system, USA), using a capillary column with fused silica and a flame-ionized detector (FID). Identifying each FAME peak was based on a 37-component mixture of FAME standards (Supelco). The recyclability of the membrane was checked by measuring the permeation flux and the separation efficiency in each cycle. The separation efficiency was determined by GC analysis. In each cycle, the membrane was gently washed with DI water for a few seconds and dried for 30 min in ambient condition before being reused.

RESULTS AND DISCUSSION

1. Synthesis of pHEMA Polymeric Film Via piCVD

When a liquid mixture is poured on a membrane surface, the heavier components in the mixture will sediment and contact the membrane first. Therefore, choosing a heavier phase as the permeate phase is generally useful to permeate the heavier phase out through the membrane by gravity. For the separation of the lipid-containing hexane phase from the microalgae culture medium, we fabricated a pHEMA-coated, water-permeating membrane via the piCVD process. Vaporized HEMA was injected into a piCVD chamber, and the injected monomers were adsorbed on the cooled substrate. By UV irradiation at a peak wavelength of 254 nm, both carbonyl groups in the adsorbed and vaporized HEMA decompose into self-initiated radicals (HEMA*), triggering the free-radical polymerization of HEMA directly on the surface of the SUS membrane (Fig. 1(a)) [35,43]. In this one-step manner, a cross-linked pHEMA-coated SUS membrane was fabricated. This membrane was then applied to the separation of a lipid-in-hexane phase from a culture medium phase, where the culture medium phase could be drained selectively through the membrane by a gravity-driven method (Fig. 1(b)).

To confirm the polymerization of HEMA, the Fourier transform-infrared (FT-IR) spectra of the monomer and the polymer synthesized by piCVD were investigated (Fig. 2(a)). The broad peak at

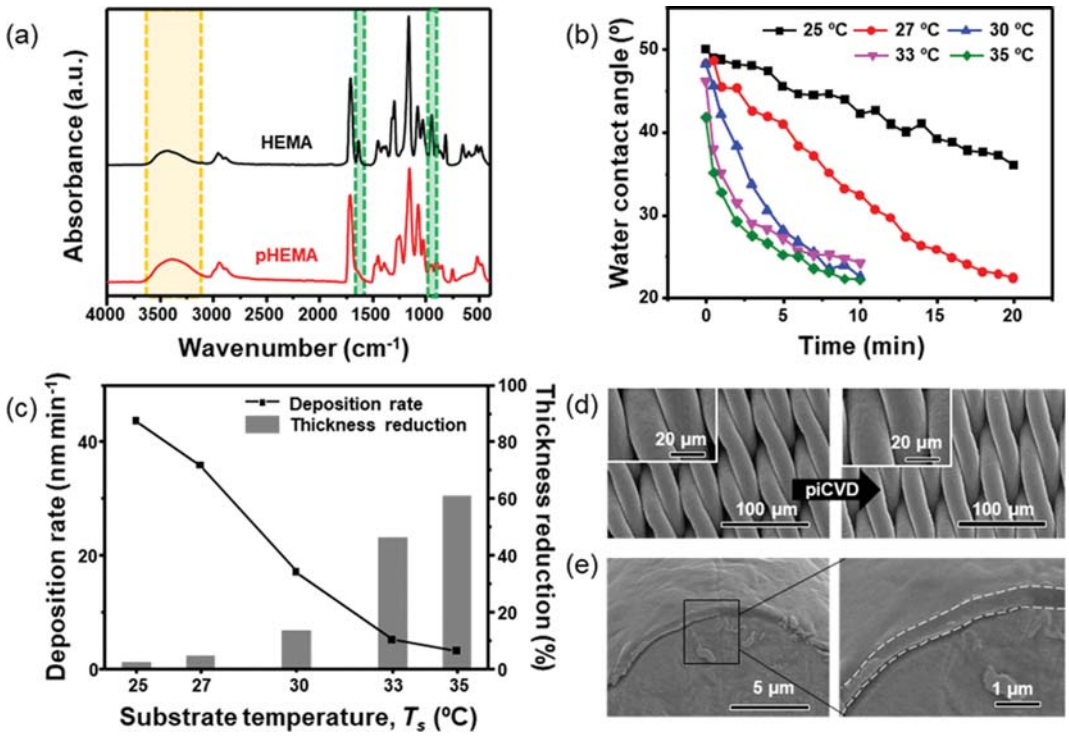

Fig. 2. (a) The FT-IR spectra of monomer, HEMA (top, black), and polymer, pHEMA (down, red). The yellow area represents the presence of the hydroxyl group and the green shades correspond to the characteristic peaks for the vinyl group. (b) The time dependent water contact angle variation of the pHEMA-coated surface deposited at a T_s of 25, 27, 30, 33, 35 °C, respectively. (c) The thickness reduction of pHEMA-coated surface deposited at each T_s after soaking in DI water for 24 hrs (left, column) and the piCVD deposition rate vs the substrate temperature (right, line) (d) SEM images of SUS membrane before (left) and after (right) the coating of pHEMA via piCVD. Each inset image shows an enlarged view of the corresponding left image. (e) Cross-sectional SEM images of 550 nm-thick pHEMA-coated membrane (left) and an enlarged view of the black square box (right).

3,400 cm^{-1} representing the hydroxyl group in HEMA was well preserved in both FT-IR spectra, indicating that the hydroxyl group was not damaged during the piCVD process [44]. On the other hand, the peak intensities corresponding to the vinyl group at 1,634 cm^{-1} (stretching) and 900 cm^{-1} (bending) detected in the HEMA spectrum decreased dramatically in the pHEMA spectrum, confirming the conversion of the HEMA monomer to pHEMA polymer [45]. The FT-IR spectra demonstrated that the HEMA underwent a free-radical polymerization to form pHEMA with minimal loss of the characteristic hydroxyl functionality through the piCVD process.

To obtain a water-permeating membrane, we employed a water-absorbing surface capable of permeating water efficiently. At the same time, the absorbed water can form a thin, water skin layer at the membrane surface, which can prevent the permeation of oil through the water-absorbing membrane [46,47]. In addition, the surface properties must survive the attack from organic solvents as well as culture media containing various constituents. Moreover, microalgal bio-lipid separation must be secured with reliable separation performance. Due to its polar hydroxyl group, pHEMA is highly hydrophilic and hygroscopic. For reliable membrane-based separation, the solvent resistance of the hydrophilic polymer must be ensured so that the polymer remains intact even with continuous contact with various kinds of solvents. Cross-linking of the polymer is an efficient way to prevent solvent-originated damage [34,37]. It has been reported that in the course of self-initiated photo-polymerization of HEMA by the piCVD method, the activated pendent carbonyl groups in the pHEMA polymer chain can induce cross-linking of the pHEMA coating by producing dimethacrylate cross-linking sites via transesterification or etherification, which substantially stabilizes the piCVD pHEMA film against attack by organic solvents [35,48,49].

The deposition condition was optimized to maximize the chemical stability of the pHEMA while retaining maximum hydrophilicity of the polymer. In the course of the optimization procedure, the substrate temperature (T_s) was found to be an important factor governing the hydrophilicity of the pHEMA [35]. By changing T_s from 25 °C to 35 °C, the amount of adsorbed monomer on the membrane surface could be controlled while maintaining all the other process conditions the same [50]. The time dependent variation of water contact angles (WCAs) on the pHEMA surfaces at each T_s condition was monitored (Fig. 2(b)). In all samples, the WCA decreased with time, demonstrating that the pHEMA surface absorbed water and became more hydrophilic. Interestingly, the pHEMA surface deposited at a higher T_s showed a rapid decrease in the WCA with the lapse of time, showing that the pHEMA with the higher T_s is more hygroscopic and hydrophilic. The pHEMA surface with a T_s above 30 °C showed a saturated WCA at around 20° in 10 min. The WCA of the pHEMA surface with a T_s of 27 °C also reached a WCA of 21° in 20 min, indicating that the surface became sufficiently hydrophilic. On the other hand, the pHEMA surface with a T_s of 25 °C is less hydrophilic. Although a decrease in the WCA was observed, the slow, linear WCA decrease of this surface strongly indicates that the pHEMA deposited at 25 °C was heavily cross-linked, which reduced the hydrophilicity of the pHEMA surface. Fig. 2(c) shows the thickness reduction of each pHEMA film after soaking the film in water for 24 h, demonstrating the underwater stability of pHEMA. The thickness reduction of pHEMA with T_s of 25 and 27 °C was less than 4.5%, while, the thickness reduction of the polymer film deposited at above 30 °C was considerable, indicating that pHEMA with a T_s below 27 °C was well-crosslinked and provided long-term underwater stability, which is critical for reliable membrane-based separation. On the other hand, the pHEMA films deposited at above 30 °C were prone to damage by water. The increased T_s decreases the amount of adsorbed monomer, which is directly related to a decrease in the surface concentration of the polymerization reaction, and thus a reduction in the cross-linking reaction to form pHEMA with a lower degree of cross-linking, consistent with a previous report [35]. Analogously, the deposition rate was also decreased with increased T_s due to the decreased surface concentration of HEMA monomer (Fig. 2(c)). Based on this analysis, we determined that the pHEMA with a T_s of 27 °C is the optimum surface with sufficient hydrophilicity and excellent underwater stability, which are important characteristics for membrane applications.

In the piCVD process, the pHEMA was synthesized from the monomers adsorbed on the substrates, where the polymer film grows from the substrates surface, leading to conformal coverage of 550 nm-thick pHEMA on the SUS membrane. Therefore, the porous membrane structure was well preserved, as shown in Fig. 2(d) and 2(e). The scanning electron microscopy (SEM) images before and after the coating showed nearly an identical structure. No apparent pore clogging or damage of the SUS membrane was observed. The pore diameters of the membrane before and after pHEMA coating were further measured by capillary flow porometer. The mean pore diameters of bare and pHEMA-coated membrane were 8.82 μm and 8.72 μm, respectively, demonstrating no decrease in pore size after piCVD coating. The pore size distribution showed that 92.9% and 88.3% of the bare and pHEMA-coated membrane, respectively, were in the range from 8 μm to 9 μm in pore diameters (Fig. S1. in Supporting Information). In addition, the pHEMA film on Si wafer showed a smooth surface morphology with a root-mean-squared roughness (R_q) of *ca* 3.2 nm (Fig. S2. in Supporting Information). The roughness is smaller than the porous structure of the membrane, which is most likely due to the planarization effect appeared in piCVD [51-53].

2. Wettability Analysis and Water Absorbing Property of the pHEMA-coated Membrane

To achieve oil/water separation, selective wettability is pivotally important for membrane-based separation. First, the WCA of the bare membrane was 93.1° while pHEMA-coated membrane became completely wettable within 30 s (Fig. 3(a)), due to its outstanding hygroscopic property as well as the highly textured structure of the SUS membrane. The oil contact angle (OCA) of the pHEMA-coated membrane soaked in water was also measured to check the underwater oil-repellency of the membrane surface. The apparent underwater OCA of the pHEMA-coated membrane was 147.1° (Fig. 3(b)), which suggests that the pHEMA-coated SUS membrane is highly hydrophilic and underwater-oleophobic. Consequently, water permeated through the membrane, while oil was rejected from the membrane, due to the sharp contrast in the wettability of water and oil on the membrane.

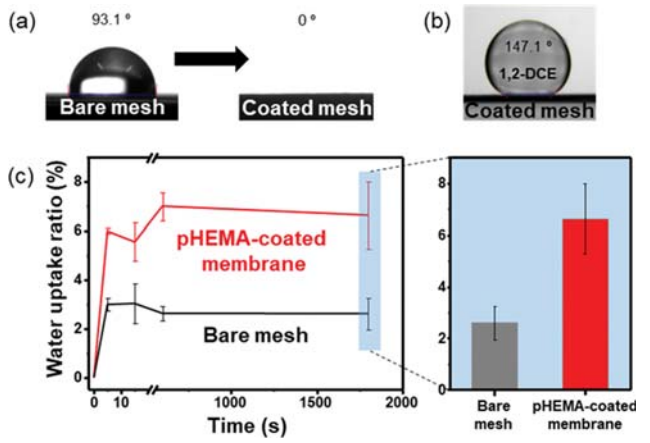

Fig. 3. (a) The water contact angles of SUS membrane before (left) and after (right) the pHEMA coating via piCVD. (b) The underwater oil contact angle of pHEMA-coated membrane. 1,2-dichloroethane dyed with Oil red O was used for better visualization. (c) The water uptake ratio of pHEMA-coated membrane (top, red) and bare membrane (down, black). The blue-shaded graph shows an enlarged view of the water uptake ratio at 30 min.

The hygroscopic property of the pHEMA-coated membrane, which is mainly responsible for the excellent water permeability and underwater-oleophobicity, was measured quantitatively by checking the swelling ratio of the pHEMA film. The pHEMA-coated membrane absorbed water 2.5 times than the bare SUS membrane and the swelling ratio was rapidly saturated within 10 min (Fig. 3(c)). Since the bare SUS material is incapable of absorbing water, about 3% of water uptake observed with the bare SUS membrane is mainly ascribed to water entrapment in the membrane pores due to the capillary effect. Considering this, at least 3 to 5% of water uptake is due to the absorption from the pHEMA thin film, corresponding to about 4.1-times the mass of pHEMA film coated on the membrane, consistent with previous observations [54]. It follows from the water uptake analysis that the pHEMA film deposited on the SUS membrane was thin enough to preserve the porous structure of the membrane, but it can also absorb a sufficient amount of water to impart excellent hydrophilicity and underwater-oleophobicity to the membrane surface.

To confirm the chemical stability against other solvents as well as water, the WCA variation of the pHEMA-coated membrane was monitored before and after treating the surface-modified membrane with various kinds of solvents. For this purpose, the pHEMA-coated membrane was soaked in various solvents such as deionized water (DI water), isopropyl alcohol (IPA), hexane, microalgal lipid-in-hexane, and a microalgal culture medium for 24 h. All the WCAs of the 24 h-tested pHEMA-coated membrane became 0° within 30 s regardless of the solvents that were used, which is practically the same as that of the pristine membrane, confirming the outstanding chemical stability of the piCVD polymer film on the SUS membrane (Fig. S3. in Supporting Information). The adhesion of pHEMA polymeric film on SUS membrane was checked by ultra-sonication treatment in isopropyl alcohol for 60 min. As shown in Fig. S4. in Supporting Information, the optical microscopic images of the membrane did not show any sign of delamination and degradation before and after the ultra-sonication treatment. The underwater oil contact angle was also maintained, which confirms the strong adhesion onto the membrane. The excellent chemical and mechanical stability of the pHEMA-coated membrane is critical to achieve reliable, efficient bio-lipid separation.

3. Separation of Olive Oil-in-hexane from Water

The hydrophilic and underwater-oleophobic pHEMA-coated membrane was applied to the separation of a model mixture to check its separation performance. The model mixture was com-

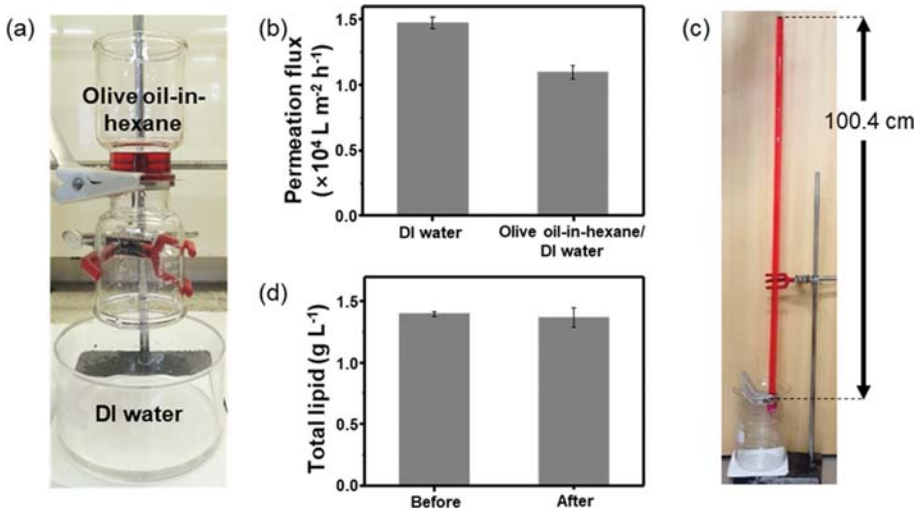

Fig. 4. (a) Photograph showing the experimental setup for the separation of olive oil-in-hexane and DI water by pHEMA-coated membrane. (b) The permeation flux of DI water only and the olive oil-in-hexane/DI water mixture through the pHEMA-coated membrane. (c) Photograph of intrusion pressure of olive oil-in-hexane on pHEMA-coated membrane. The maximum height was 100.4 cm. The olive oil-in-hexane phase was dyed with Oil red O for better visualization. (d) The olive oil concentration in hexane before and after the separation, estimated by total lipid measurement.

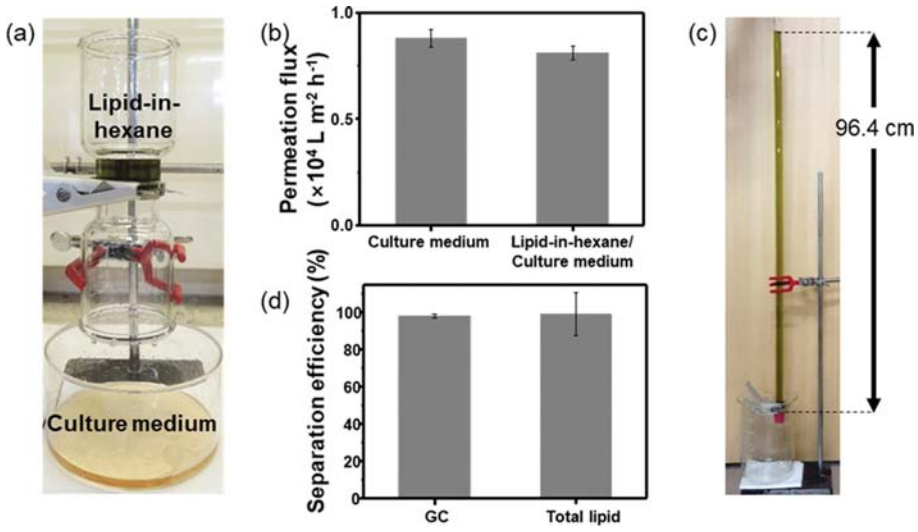

Fig. 5. (a) Photograph of the experimental setup for the separation of lipid-in-hexane and culture medium by pHEMA-coated membrane. (b) The permeation flux of culture medium only and lipid-in-hexane/culture medium mixture through the pHEMA-coated membrane. (c) Photograph of intrusion pressure of lipid-in-hexane on pHEMA-coated membrane, where the maximum height was 96.4 cm. (d) The separation efficiency of pHEMA-coated membrane obtained by GC analysis and total lipid measurement.

posed of olive oil-in-hexane (1.35 g L^{-1}) and DI water (30 v/v %, and the oil phase was dyed with Oil red O) was poured onto the apparatus equipped with the pHEMA-coated membrane. The olive oil-in-hexane was rejected from the membrane and remained on the membrane top while DI water completely passed through the membrane instantly to achieve complete separation solely by gravity (Fig. 4(a) and Supplementary Movie 1). The rapid but complete separation achieved from the membrane confirms the uniform, conformal coating of pHEMA that efficiently prevented oil leakage, while the pore size was well maintained to maximize the permeation flux. The average permeation flux of the pHEMA-coated membrane was 1.5×10^4 L m^{-2} h^{-1} for water and 1.1×10^4 L m^{-2} h^{-1} for the olive oil-in-hexane/DI water mixture (Fig. 4(b)), indicating that the resistance against water permeation is extremely low and a fast separation can be achieved just by the low-energy, gravity-driven method. The high permeation flux of the pHEMA-coated membrane is greatly advantageous for treating large amounts of oil/water mixtures with minimal energy input [21,55].

The oil intrusion pressure is also a crucial factor in determining the separation performance of the membrane. The intrusion pressure was obtained by measuring the maximum height of oil before any oil leakage from the membrane starts. The maximum height of olive oil-in-hexane was 100.4 cm and the estimated intrusion pressure was 6.4 kPa, which is considerably high compared to a previous report (Fig. 4(c)) [56]. The excellent underwater oil-repellency of the pHEMA thin film efficiently prevented oil leakage from the membrane.

To quantify the separation efficiency, the amount of oil leakage into the water permeate phase was measured by a total lipid analysis. The olive oil concentrations before and after the separation were practically identical (Fig. 4(d)). In addition, the water content in the oil phase was measured by the Karl Fischer method to check the water content remains in the rejected oil phase after the separation. The water content in the residual oil phase after the separation was extremely low, about 0.08%, which was close to the water content (0.06%) in pristine olive oil-in-hexane (Fig. S5. in Supporting Information).

4. Separation of Lipid-in-hexane from Culture Media

Finally, the cross-linked pHEMA-coated SUS membrane was employed to separate microalgal bio-lipids from a culture medium. The bio-lipid separation was carried out in the same manner as the model mixture separation described above. As expected, the bio-lipids were also separated completely from the culture medium using the pHEMA-coated membrane driven solely by gravity (Fig. 5(a)). The lipid-in-hexane phase was rejected from the membrane, while the culture medium permeated through the membrane (Supplementary Movie 2). The average permeation flux of the culture medium through the pHEMA-coated membrane was 8.1×10^3 L m^{-2} h^{-1} and the average permeation flux for the bio-lipid-in-hexane/culture medium mixture was 6.5×10^3 L m^{-2} h^{-1} (Fig. 5(b)), which was also quite high for gravity-driven flux. The lipid-in-hexane intrusion pressure of the membrane was 6.1 kPa, corresponding to a height of 96.4 cm in the lipid-in-hexane column (Fig. 5(c)). The separation efficiency was estimated by a gas chromatography (GC) analysis and total lipid measurement. The average separation efficiency obtained by the GC analysis and the total lipid measurement was 98.0% and 98.8%, respectively (Fig. 5(d)), confirming the excellent separation efficiency of the pHEMA-coated membrane-based separation. The water content of lipid-in-hexane before and after separation was obtained by the Karl Fischer method, and both showed an extremely low value of 0.08%, confirming the excellent separation efficiency (Fig. S6. in Supporting Information).

Furthermore, the reusability of the pHEMA-coated membrane was checked by measuring the separation efficiency and permeation flux in each cycle. To realize a sustainable and effective bio-lipid separation process, excellent membrane performance should be retained for repeated use. The pHEMA-coated membrane showed

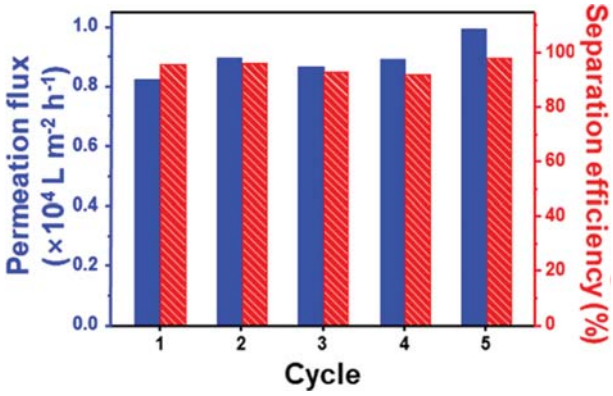

Fig. 6. Permeation flux for lipid-in-hexane and culture medium mixture (blue) and the separation efficiency (red) with respect to the reuse cycle, obtained by GC analysis.

no significant degradation of permeation flux or separation efficiency, as determined by the GC analysis, after five iterations of reuse (Fig. 6), due to the improved mechanical chemical stability of the cross-linked hydrogel-coated SUS membrane with excellent hydrophilic and underwater-oleophobic properties.

CONCLUSION

A hydrogel-coated membrane was fabricated via piCVD in a one-step manner and was used to separate microalgal bio-lipids directly from the culture medium. The selective wettability of the oil and water phase on the membrane, originating from the outstanding hydrophilicity and underwater-oleophobicity of the cross-linked pHEMA surface, led to complete separation of the bio-lipid mixture with excellent separation performance and enlarged permeation flux, achieved solely by a low-energy, gravity-driven separation method. Moreover, the mechanical durability of the SUS membrane coupled with the chemical stability of the cross-linked pHEMA thin film enabled repeated use of separation membrane without sacrificing the separation performance. The scalable strategy using the hydrophilic membrane for bio-lipid mixture separation will be useful to reduce the total energy consumption in dewatering processes.

NOTES

The authors declare no competing financial interest.

ACKNOWLEDGEMENTS

This work was supported by the Advanced Biomass R&D Center (ABC) of Global Frontier Project funded by the Ministry of Science, ICT and Future Planning (2010-0029728).

SUPPORTING INFORMATION

Additional information as noted in the text. This information is available via the Internet at http://www.springer.com/chemistry/journal/11814.

REFERENCES

1. H. Lund, *Energy*, **32**, 912 (2007).
2. M. Dresselhaus and I. Thomas, *Nature*, **414**, 332 (2001).
3. L. Lin, C. S. Zhou, S. Vittayapadung, X. Q. Shen and M. D. Dong, *Appl. Energy*, **88**, 1020 (2011).
4. Y. C. Sharma and B. Singh, *Renew. Sust. Energ. Rev.*, **13**, 1646 (2009).
5. A. E. Atabani, A. S. Silitonga, I. A. Badruddin, T. Mahlia, H. Masjuki and S. Mekhilef, *Renew. Sust. Energ. Rev.*, **16**, 2070 (2012).
6. A. L. Ahmad, N. H. M. Yasin, C. J. C. Derek and J. K. Lim, *Renew. Sust. Energ. Rev.*, **15**, 584 (2011).
7. I. Rawat, R. R. Kumar, T. Mutanda and F. Bux, *Appl. Energy*, **103**, 444 (2013).
8. Y. Chisti, *Biotechnol. Adv.*, **25**, 294 (2007).
9. S. Wu, L. R. Song, M. Sommerfeld, Q. Hu and W. Chen, *Fuel*, **197**, 467 (2017).
10. L. Lardon, A. Helias, B. Sialve, J. P. Steyer and O. Bernard, *Environ. Sci. Technol.*, **43**, 6475 (2009).
11. N. Uduman, Y. Qi, M. K. Danquah, G. M. Forde and A. Hoadley, *J. Renew. Sustain. Ener.*, **2**(1), 012701 (2010).
12. M. Rizwan, J. H. Lee and R. Gani, *Appl. Energy*, **150**, 69 (2015).
13. S. Y. Choy, *Algal Res.* (2017), DOI:10.1016/j.algal.2017.1011.1012.
14. H. Taher, S. Al-Zuhair, A. H. Al-Marzouqi, Y. Haik and M. Farid, *Biomass Bioenergy*, **66**, 159 (2014).
15. G. Yoo, W.-K. Park, C. W. Kim, Y.-E. Choi and J.-W. Yang, *Bioresour. Technol.*, **123**, 717 (2012).
16. W. M. A. W. Mahmood, C. Theodoropoulos and M. Gonzalez-Miquel, *Green Chem.*, **19**, 5723 (2017).
17. A. Silve, I. Papachristou, R. Wüstner, R. Sträßner, M. Schirmer, K. Leber, B. Guo, L. Interrante, C. Posten and W. Frey, *Algal Res.*, **29**, 212 (2018).
18. Z. Xue, Y. Cao, N. Liu, L. Feng and L. Jiang, *J. Mater. Chem. A*, **2**, 2445 (2014).
19. M. Padaki, R. S. Murali, M. S. Abdullah, N. Misdan, A. Moslehyani, M. A. Kassim, N. Hilal and A. F. Ismail, *Desalination*, **357**, 197 (2015).
20. Z. X. Xue, S. T. Wang, L. Lin, L. Chen, M. J. Liu, L. Feng and L. Jiang, *Adv. Mater.*, **23**, 4270 (2011).
21. K. Rohrbach, Y. Li, H. Zhu, Z. Liu, J. Dai, J. Andreasen and L. Hu, *Chem. Commun. (Camb)*, **50**, 13296 (2014).
22. M. W. Lee, S. An, S. S. Latthe, C. Lee, S. Hong and S. S. Yoon, *ACS Appl. Mater. Inter.*, **5**, 10597 (2013).
23. J. Li, L. Yan, H. Li, J. Li, F. Zha and Z. Lei, *RSC Adv.*, **5**, 53802 (2015).
24. M. J. Kwak, Y. Yoo, H. S. Lee, J. Kim, J. W. Yang, J. I. Han, S. G. Im and J. H. Kwon, *ACS Appl. Mater. Inter.*, **8**, 600 (2016).
25. F. Smedes, *Analyst*, **124**, 1711 (1999).
26. M. D. Antezana Zbinden, B. S. M. Sturm, R. D. Nord, W. J. Carey, D. Moore, H. Shinogle and S. M. Stagg-Williams, *Biotechnol. Bioeng.*, **110**, 1605 (2013).
27. R. Halim, B. Gladman, M. K. Danquah and P. A. Webley, *Bioresour. Technol.*, **102**, 178 (2011).
28. Q. L. Ma, H. F. Cheng, A. G. Fane, R. Wang and H. Zhang, *Small*, **12**, 2186 (2016).
29. W. Zhang, Y. Cao, N. Liu, Y. Chen and L. Feng, *RSC Adv.*, **4**, 51404 (2014).

30. Z.-Y. Luo, K.-X. Chen, Y.-Q. Wang, J.-H. Wang, D.-C. Mo and S.-S. Lyu, *J. Phys. Chem. C*, **120**, 12685 (2016).
31. G. Wang, Y. He, H. Wang, L. Zhang, Q. Yu, S. Peng, X. Wu, T. Ren, Z. Zeng and Q. Xue, *Green Chem.*, **17**, 3093 (2015).
32. F. Zhang, W. B. Zhang, Z. Shi, D. Wang, J. Jin and L. Jiang, *Adv. Mater.*, **25**, 4192 (2013).
33. M. Sun, Q. Y. Wu, J. Xu, F. He, A. P. Brown and Y. M. Ye, *J. Mater. Chem. B*, **4**, 2669 (2016).
34. M. Joo, J. Shin, J. Kim, J. B. You, Y. Yoo, M. J. Kwak, M. S. Oh and S. G. Im, *J. Am. Chem. Soc.*, **139**, 2329 (2017).
35. S. H. Baxamusa, L. Montero, J. M. Dubach, H. A. Clark, S. Borros and K. K. Gleason, *Biomacromolecules*, **9**, 2857 (2008).
36. J. B. You, Y. Yoo, M. S. Oh and S. G. Im, *ACS Appl. Mater. Inter.*, **6**, 4005 (2014).
37. M. J. Kwak, M. S. Oh, Y. Yoo, J. B. You, J. Kim, S. J. Yu and S. G. Im, *Chem. Mater.*, **27**, 3441 (2015).
38. B. J. Kim, D. Han, S. Yoo and S. G. Im, *Korean J. Chem. Eng.*, **34**, 892 (2017).
39. F. Zhang, W. B. Zhang, Z. Shi, D. Wang, J. Jin and L. Jiang, *Adv. Mater.*, **25**, 4192 (2013).
40. X. Zhao, Y. Su, Y. Liu, Y. Li and Z. Jiang, *ACS Appl. Mater. Inter.*, **8**, 8247 (2016).
41. L. Liu, C. Chen, S. Yang, H. Xie, M. Gong and X. Xu, *Phys. Chem. Chem. Phys.*, **18**, 1317 (2016).
42. A. Gallina, N. Stocco and F. Mutinelli, *Food Control*, **21**, 942 (2010).
43. E. Abrahamson, J. Littler and K. P. Vo, *J. Chem. Phys.*, **44**, 4082 (1966).
44. K. Chan and K. K. Gleason, *Langmuir*, **21**, 8930 (2005).
45. G. M. Jeong, H. Seong, Y. S. Kim, S. G. Im and K. J. Jeong, *Polym. Chem.*, **5**, 4459 (2014).
46. X. Zheng, Z. Guo, D. Tian, X. Zhang, W. Li and L. Jiang, *ACS Appl. Mater. Inter.,* **7**, 4336 (2015).
47. P. C. Chen and Z. K. Xu, *Sci. Rep.*, **3**, 2776 (2013).
48. J. Lee, T. Aoai, S. i. Kondo, N. Miyagawa, S. Takahara and T. Yamaoka, *J. Polym. Sci., Part A: Polym. Chem.*, **40**, 1858 (2002).
49. M. Vasilopoulou, S. Boyatzis, I. Raptis, D. Dimotikalli and P. Argitis, *J. Mater. Chem.*, **14**, 3312 (2004).
50. K. K. S. Lau and K. K. Gleason, *Macromolecules*, **39**, 3688 (2006).
51. S. Lee, H. Seong, S. G. Im, H. Moon and S. Yoo, *Nat. Commun.*, **8**, 725 (2017).
52. Y. I. Lee, N. J. Jeon, B. J. Kim, H. Shim, T. Y. Yang, S. I. Seok, J. Seo and S. G. Im, *Adv. Energy Mater.*, 1701928 (Online Version) (2017).
53. R. Bakker, V. Verlaan, C. Van der Werf, J. Rath, K. Gleason and R. Schropp, *Surf. Coat. Technol.*, **201**, 9422 (2007).
54. P. H. Corkhill, A. M. Jolly, C. O. Ng and B. J. Tighe, *Polymer*, **28**, 1758 (1987).
55. M. Tao, L. Xue, F. Liu and L. Jiang, *Adv. Mater.*, **26**, 2943 (2014).
56. S. J. Gao, Z. Shi, W. B. Zhang, F. Zhang and J. Lin, *ACS Nano*, **8**, 6344 (2014).

Supporting Information

A hydrogel-coated membrane for highly efficient separation of microalgal bio-lipid

Jihye Shin*, Hogi Kim*, Heeyeon Moon*, Moo Jin Kwak*, Seula Oh*, Youngmin Yoo*, Eunjung Lee*, Yong Keun Chang*,,†, and Sung Gap Im*,†**

*Department of Chemical and Biomolecular Engineering, KAIST, Daejeon 34141, Korea
**Advanced Biomass R&D Center, Daejeon 34141, Korea
(*Received 20 November 2017 • accepted 23 February 2018*)

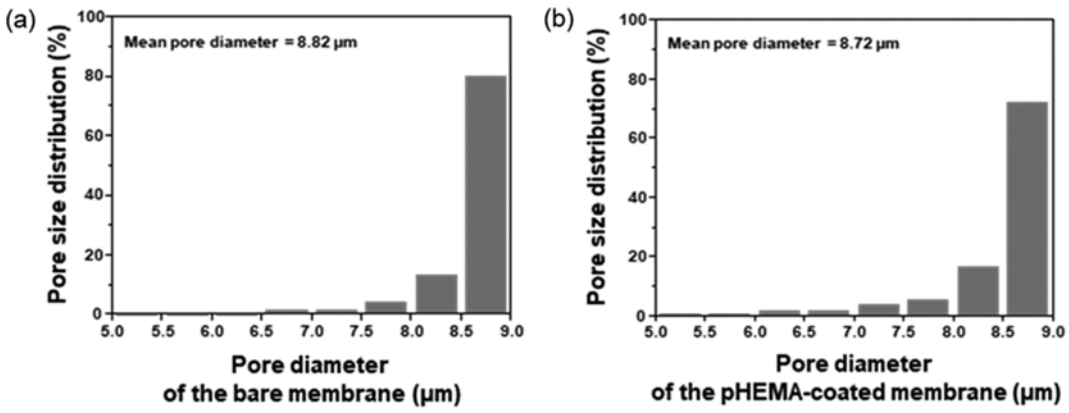

Fig. S1. The pore size distribution and pore diameter of (a) bare membrane and (b) pHEMA-coated membrane.

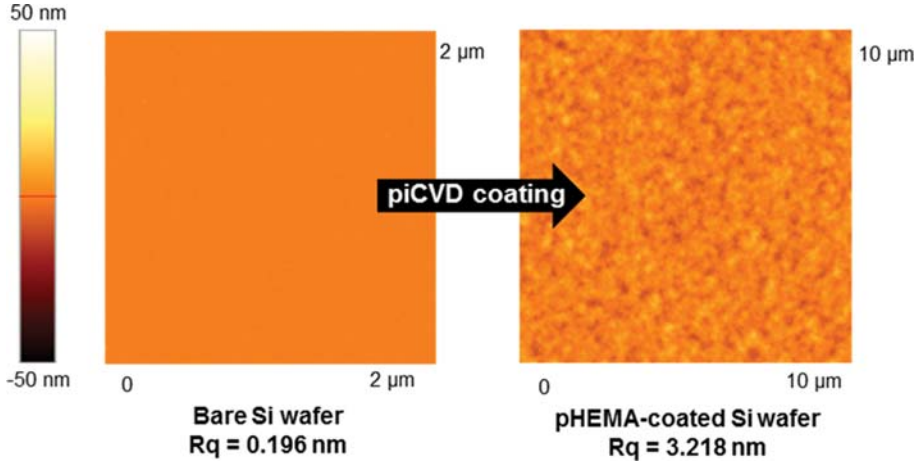

Fig. S2. AFM images of bare Si wafer (left) and piCVD pHEMA-coated Si wafer (right).

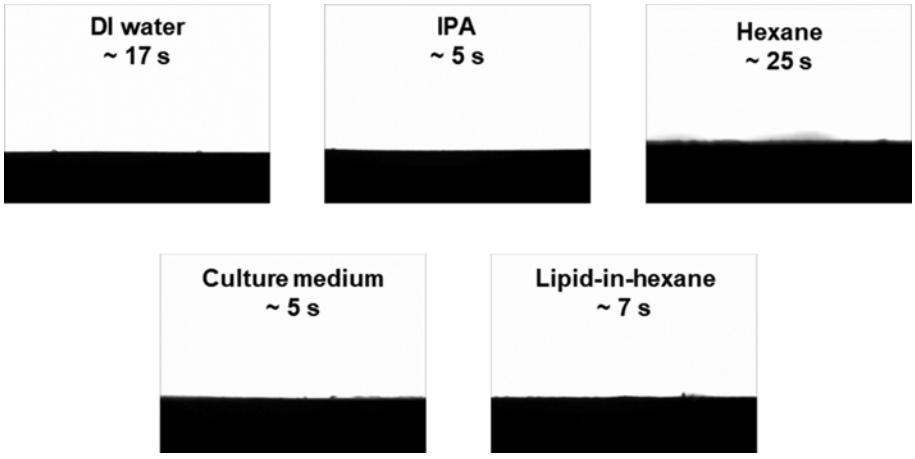

Fig. S3. The WCAs of solvent-incubated pHEMA-coated membranes for 24 hrs. All of the solvent-incubated membranes show super-hydrophilic property and each time represents the time to reach complete spreading of water droplet.

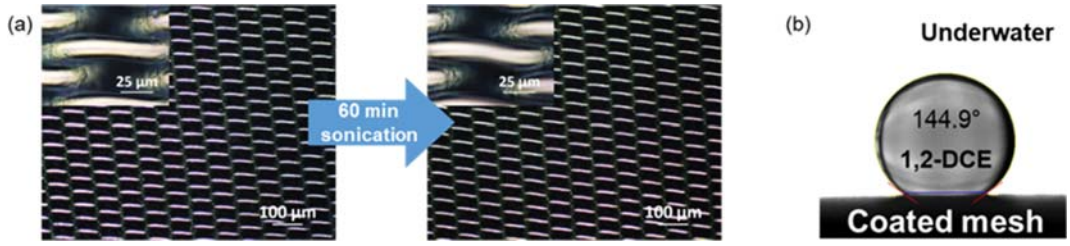

Fig. S4. (a) The optical microscopic images of the pHEMA-coated mesh before (left) and after (after) the ultra-sonication treatment in isopropyl alcohol for 60 min. Each inset is an enlarged view of the membrane. (b) Underwater oil contact angle (144.9°) on pHEMA-coated mesh after ultra-sonication. 1,2-Dichloroethane (1,2-DCE) was used.

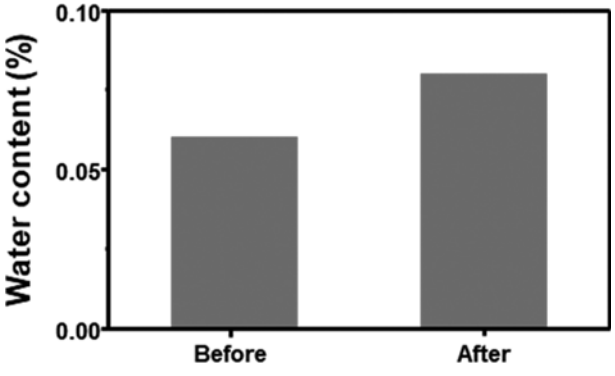

Fig. S5. The water content in olive oil-in-hexane phase before and after the membrane separation, estimated by Karl-Fischer method.

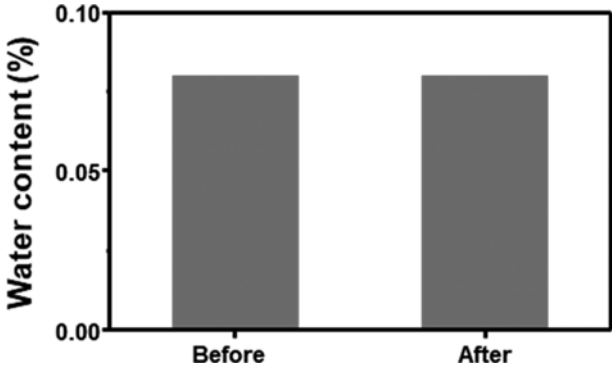

Fig. S6. The water content in lipid-in-hexane phase before and after the microalgal lipid separation, estimated by Karl-Fischer method.